On the use of a rounded sonotrode for the welding of thermoplastic composites

Jongbloed, B.C.P.; Teuwen, Julie J.E.; Fernandez Villegas, I.

DOI
10.1016/j.jajp.2023.100144

Publication date
2023

Document Version
Final published version

Published in
Journal of Advanced Joining Processes

Journal of Advanced Joining Processes 7 (2023) 100144

Contents lists available at ScienceDirect

Journal of Advanced Joining Processes

journal homepage: www.sciencedirect.com/journal/journal-of-advanced-joining-processes

On the use of a rounded sonotrode for the welding of thermoplastic composites

Bram Jongbloed [a,b,*], Julie Teuwen [a], Irene Fernandez Villegas [a]

[a] Department of Aerospace Structures and Materials, Faculty of Aerospace Engineering, Delft University of Technology, Kluyverweg 1, Delft 2629 HS, the Netherlands
[b] SAM XL, TU Delft Campus, Rotterdamseweg 382C, Delft 2629 HG, the Netherlands

ARTICLE INFO

Keywords:
Fusion bonding
Continuous ultrasonic welding
Consolidation
Joining
CF/PPS

ABSTRACT

Continuous ultrasonic welding is an attractive welding technique for thermoplastic composite structures. In this process, a metallic sonotrode connected to a piezoelectric transducer and to a press moves along the parts to be welded applying ultrasonic vibrations and a static welding force on the welding overlap. Thus far, the research carried out on this topic makes use of sonotrodes featuring a flat contact surface with the parts to be welded, which limits the use of the process to the welding of overlaps with no curvature in the welding direction. With the final aim of assessing whether this process can also be applied to curved structures, this paper explores the feasibility of using a rounded sonotrode for continuous ultrasonic welding of thermoplastic composites. The main conclusions drawn from the results obtained in this research is that it is indeed possible to continuously weld thermoplastic composite panels with a rounded sonotrode and that high-quality welds can be obtained from such a process. Furthermore, the use of a rounded sonotrode has the positive effect of lowering the temperatures at the welding interface as well as the temperatures within the adherends. On the other hand, the use of such sonotrode leads to a decreased, although still competitive, welding speed and, potentially, an increased welding force, thereby setting boundary conditions that need to be considered for each specific application.

Introduction

The increasing demands for more sustainable aircraft, reduced costs and high cycle times, encourage the fast introduction of thermoplastic composites in aircraft structures. A perfect example of this is the Multifunctional Fuselage Demonstrator (MFFD) within the framework of the Clean Sky 2 Joint Undertaking (Clean Aviation, 2022; Gardiner). The MFFD, with a length and diameter of 8.5 m and 4.0 m, respectively is the first and largest fully thermoplastic composite aircraft structure ever built. This demonstrator showcases precisely those technologies that make thermoplastic composites so versatile and cost effective like, press forming, continuous compression moulding, injection moulding, and welding. These technologies rely on the characteristic of the thermoplastic matrix to melt upon heating, and solidify when cooled down.

The most interesting welding technologies for thermoplastic composites are induction, resistance, and ultrasonic welding (Ageorges et al., 2001; Benatar and Gutowski, 1986; Yousefpour et al., 2004). The latter is typically regarded as the fastest and most energy efficient process of all of them (Villegas et al., 2013). Ultrasonic welding relies on the introduction of high-frequency, low-amplitude mechanical vibrations into the composite parts to be welded by means of a sonotrode (Grewell et al., 2003). Using of a so-called energy director (ED), e.g. a polymer film or mesh, helps focus heat generation at the welding interface (Benatar et al., 1989; Villegas, 2019). Heat is generated by means of frictional heating between the surfaces of the ED and the parts and through viscoelastic heating (Potente, 1984; Zongbo Zhang et al., 2010). Due to its typically lower stiffness, the ED undergoes higher cyclic straining under the ultrasonic vibration and hence has a higher viscoelastic heat generating capacity than the composite parts.

Two ultrasonic welding processes can be used for welding of thermoplastic composite structures, namely sequential spot welding and continuous welding. Sequential spot welding produces multi-spot welded joints (Zhao et al., 2018; 2019) and hence a discontinuous welded seam. On the contrary, in continuous ultrasonic welding a continuous seam is established by continuously moving the sonotrode along the welding overlap (Senders et al., 2016). Both processes consist of a vibration phase and a consolidation phase. During the vibration phase heat is generated by means of the application of the ultrasonic vibrations. During the consolidation phase the joint cools down and solidifies under pressure. In the spot welding process the sonotrode itself provides

* Corresponding author at: SAM XL, TU Delft Campus, Rotterdamseweg 382C, Delft 2629 HG, the Netherlands
E-mail address: B.C.P.Jongbloed@tudelft.nl (B. Jongbloed).

https://doi.org/10.1016/j.jajp.2023.100144
Received 30 November 2022; Received in revised form 6 March 2023; Accepted 26 March 2023
Available online 29 March 2023

the consolidation pressure from the end of the vibration phase. In the continuous process, however, a separate consolidation shoe, referred to as consolidator hereafter, is required to apply the consolidation pressure and ensure high weld quality (Jongbloed et al., 2022). State-of-the-art continuous ultrasonic welding typically makes use of a rectangular sonotrode with hence a flat contact surface with the parts to be welded (Jongbloed et al., 2020a,b, 2021, 2022). Using this type of sonotrode enables significantly high welding speeds (e.g., about 35 mm/s welding speed for fabric carbon fibre reinforced polyphenylene sulfide, CF/PPS Jongbloed et al., 2020a). However, this solution is only applicable to overlaps with no curvature in the welding direction, i.e., the direction of movement of the sonotrode.

With the goal of eventually applying ultrasonic welding to single-curved structures, e.g., circumferential joints in a fuselage structure, we explored in this research the feasibility of using of a rounded sonotrode for the continuous ultrasonic welding of thermoplastic composites. As part of this exploration we looked into the weld quality (voids, squeeze out, weld strength) and the welding process itself (temperature evolution at the weld line and within the adherends, energy and power). We then compared these results to those obtained with a state-of-the-art rectangular sonotrode and published in our earlier paper (Jongbloed et al., 2021b). As a first step in this novel line of research, the adherends were kept flat, nevertheless the results obtained contain valuable information about the feasibility of using a continuous process for the ultrasonic welding of curved adherends.

Methodology

Material

Carbon fibre reinforced polyphenylene sulfide (CF/PPS) thermoplastic composite laminates were used in this study as material for the welding adherends. The laminates were produced by press consolidating stacks of 6 layers of powder-impregnated CF/PPS semipreg material (5 harness satin CF fabric, CF 0286 127 Tef4 43% from Toray Advanced Composites, The Netherlands) at 320 °C and 1 MPa for 20 min. The laminates had a $[0/90]_{3s}$ stacking sequence, measured 580 mm × 580 mm and had an approximate thickness of 1.85 mm upon consolidation. Adherends measuring 220 mm × 101.6 mm were water-jet cut from the consolidated laminates and degreased with isopropyl alcohol prior to the welding process. The main apparent fibre orientation was parallel to the short direction of these adherends. A 0.20 mm-thick plain woven PPS mesh with 37% open area (PPS100, PVF GmbH, Germany) was used as energy director in order to focus heat generation at the welding interface (Jongbloed et al., 2020b).

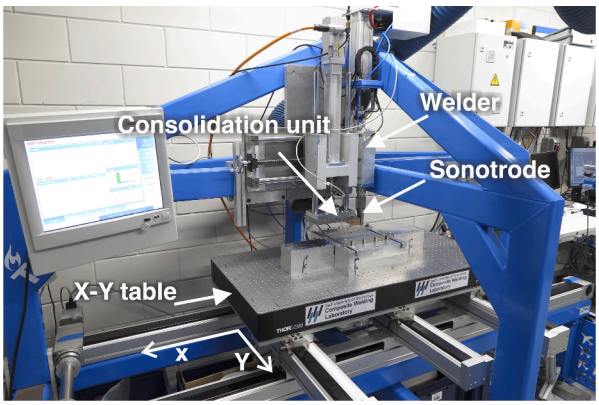

Fig. 1. Welding setup.

Welding setup and welding process

Fig. 1 shows the entire welding setup featuring a stiff frame to which the ultrasonic welder and the consolidation unit are connected, and a X-Y table on a guiding system able to move in the *x* and *y* directions at both constant and variable speed. A VE20 SLIMLINE DIALOG 6200 ultrasonic welder (Hermann Ultrasonics, Germany) operating at 20 kHz and with maximum power of 6.2 kW is used in this setup. Next to it, a custom-built consolidator is used to allow cooling down of the material under pressure after the welding process. It consists of a 1.5 kN servo press kit (YJKP, Festo, The Netherlands), a stabilization guide unit to avoid sideways deflections and a 40 mm × 30 mm consolidation block made out of copper. Note that the front of the 40 mm-long copper block is rounded (2 mm radius) on the front to ensure a smooth sliding process. The sonotrode used in this study was custom-built by Aeson (The Netherlands) and made from titanium. On the plane defined by the perpendicular axis of the sonotrode and the welding direction (Fig. 2), the cross-section of the lower portion of the sonotrode is an approximately 15 mm-wide rectangle with a 15 mm diameter rounded tip attached to it. On the plane containing the perpendicular axis of the sonotrode and normal to the welding direction, the sonotrode features a 30 mm-wide rectangular cross section (Fig. 3). The distance between the consolidation unit and the shaft of the sonotrode was kept as short as possible (i.e., 2.5 mm, see Fig. 2) for the setup to operate safely. Finally, the adherends were clamped to and aluminium base using bar clamps. The aluminium base was located and fixed to the X-Y table so that the sonotrode would mainly make contact with the 12.7 mm-long welding overlap (Fig. 3).

The welding force and amplitude of vibration were set to 1000 N and 80 μm (peak-to-peak), respectively. For such welding force, the welding pressure was approximately 43–53 MPa, with the contact area between sonotrode and material measured using carbon paper and amounting to approximately 19 mm^2 (~1.5 mm × 12.7 mm). The welding speed was set at 12 mm/s based on preliminary experiments in which, within a range between 25 and 8 mm/s, 12 mm/s was found to provide welds with fully molten ED and no signs of thermal degradation (observations on fracture surfaces). In most of the experiments, the consolidation force was set to 800 N. This resulted in 1.6 MPa consolidation pressure, which in our previous study (Jongbloed et al., 2022) was found to be sufficient to fully consolidate the same material. Some experiments were however carried out without the use of a consolidator. Their goal was to qualitatively identify regions in the material (adherends and weld line) which

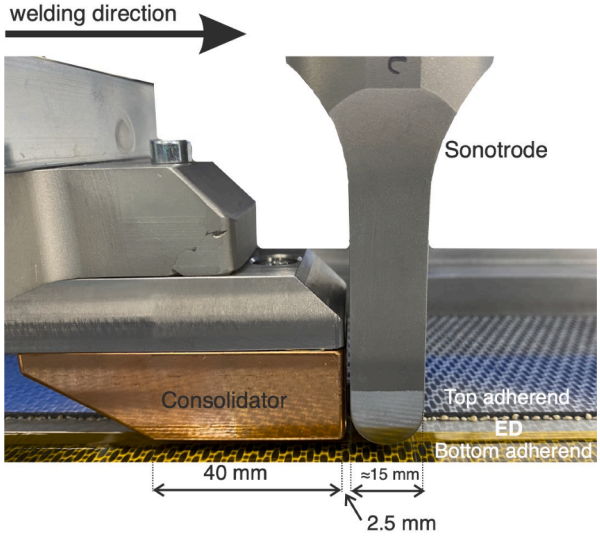

Fig. 2. Close-up of the welding setup showing the rounded sonotrode and the consolidation block.

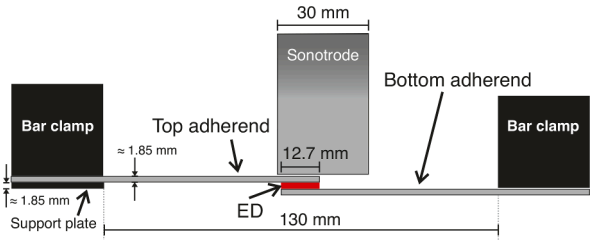

Fig. 3. Schematic placement of clamps and sonotrode.

had reached temperatures above melting, in the assumption that they would develop deconsolidation voids upon cooling.

Temperature measurements

Thin K-type thermocouples (GG220-2K-0, Tempco B.V., The Netherlands) were used to measure the temperature evolutions at the welding interface and within the adherends, while minimizing their effect on the welding process. The diameter of the thermocouple wires was 0.10 mm, while the total diameter of the sleeved wires was 0.70 mm. An analogue thermocouple signal amplifier (Adafruit AD8495) was used to simultaneously sample temperature readings at 1 kHz from a maximum of five thermocouples. A MATLAB moving average filter (10, 20 or 25 points, depending on the individual case) was used to filter out high-frequency fluctuations from the temperature data. Thermocouples placed between the bottom adherend and the energy director were used to measure the temperature evolution at the welding interface. For the measurements within the adherends, the thermocouples were inserted into 0.7 mm diameter holes drilled approximately midway through the thickness of the laminate. Note that the diameter of the hole and of the sleeved thermocouple were the same to ensure a press fit. Fig. 4 schematically shows the locations of the thermocouples used to measure temperatures at the welding interface (Configuration A), within the top adherend (plus welding interface, Configuration B) and within the bottom adherend (plus welding interface, Configuration C).

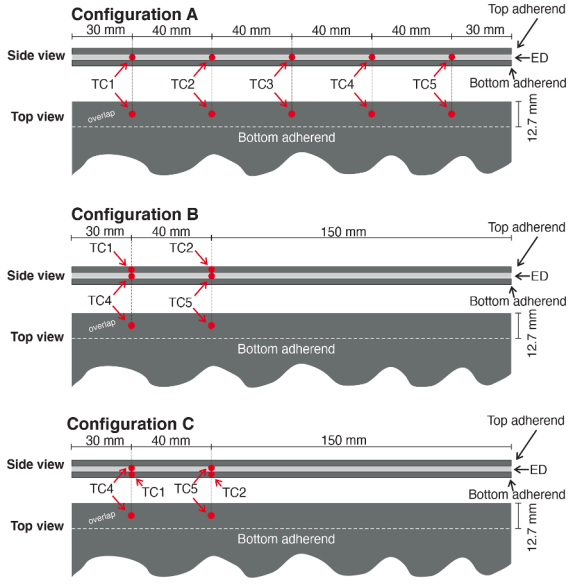

Fig. 4. Different thermocouple configurations used in this study. Configuration A: temperature evolution at five different locations at the welding interface; configuration B: temperature evolution at two locations within top adherend and welding interface; configuration C: temperature evolution at two locations within bottom adherend and welding interface.

Microscopy and mechanical tests

The welded panels were cut into six 25.4 mm-wide coupons discarding 28.8 mm at each edge of the panel. A water-cooled diamond grinder was used for this purpose. One of these coupons (coupon #3, located approximately at the centre of the welded panel) was used for cross-sectional microscopic analysis of the welded overlap. For this, the specimen was further trimmed, embedded in epoxy resin, and finally ground and polished with a Tergramin-20 polisher (Struers, Denmark). A 3D laser scanning confocal microscope (Keyence VK-X1000, Belgium) was used for inspecting the cross sections. The other five coupons were single-lap shear tested using a 250 kN Zwick/Roell universal testing machine. The grips of the testing machine were offset to minimize secondary bending. Based on the ASTM D 1002 standard, a cross-head speed of 1.3 mm/min was used in the tests and the apparent single-lap shear strength (LSS) of the welded joints was calculated as the maximum load divided by the overlap area (i.e., 25.4 × 12.7 mm^2). Fracture surfaces underwent naked-eye observation. Note that some of the coupons subjected to mechanical tests contained a thermocouple in the weldline. Our assumption is that, owing to its small dimensions, the effect of the thermocouple on the weld strength can be considered as negligible.

Test matrix

Table 1 shows an overview of the different welded joints produced in this study and the types of tests they were used for.

Results

Weld quality

Fig. 5 presents a representative cross-section micrograph of the welded joints obtained in this study showing the general state of the material at the weld line and adjacent areas in the adherends as well as the regions from which material is squeezed out at the edges of the overlap (weld line primarily). Fig. 6 shows a representative cross-section micrograph of a welded joint obtained with the absence of a consolidator to help identify the areas where enough heat was generated to melt the PPS matrix during the welding process, mostly the weld line and the first layer adjacent to the weld interface in the top adherend. From the single-lap shear strength tests on five coupons cut from a single welded panel, a weld strength of 33.5 MPa was obtained with 1.4 MPa standard deviation. The corresponding fracture surfaces are shown in Fig. 7. Fig. 8 shows a close-up from one of the coupons.

Welding process

The average power consumed by the ultrasonic welder during the welding process was approx. 270 W and the energy density, approx. 1.8 J/mm^2. The temperature evolution at the interface between bottom

Table 1
Test matrix.

TC configuration (Fig. 4)	Number of welds	Adherend size [mm × mm]	Weld length [mm]	Remarks
A	1	220 × 101.6	185	T measurements, LSS tests & cross-sectional microscopy.
A	1	220 × 101.6	185	T measurements, & cross-sectional microscopy. No consolidator.
B	1	220 × 101.6	78	T measurements only.
C	1	220 × 101.6	78	T measurements only.

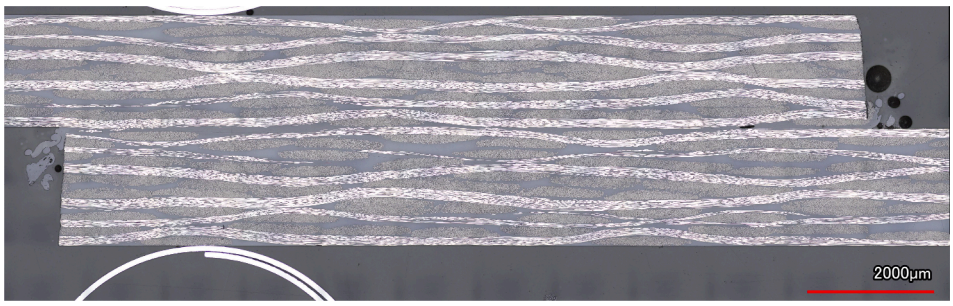

Fig. 5. Cross-sectional micrograph of continuous ultrasonic weld made using rounded sonotrode. Top adherend shown on top.

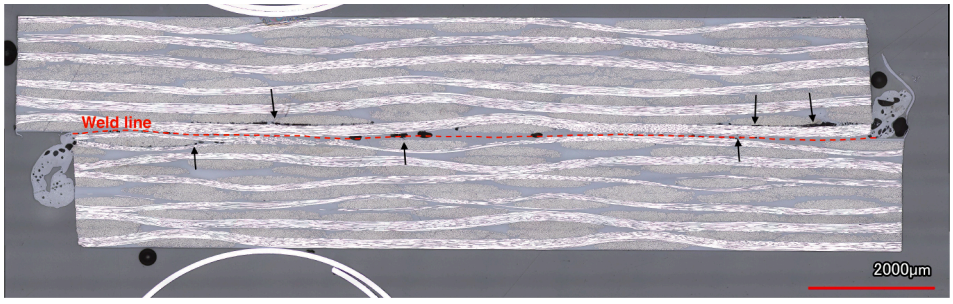

Fig. 6. Cross-sectional micrograph of continuous ultrasonic weld made using rounded sonotrode and no consolidator. Top adherend shown on top. Deconsolidation voids can be seen at the weldline as well as the first layer of the top adherend adjacent to the welding interface indicated by arrows.

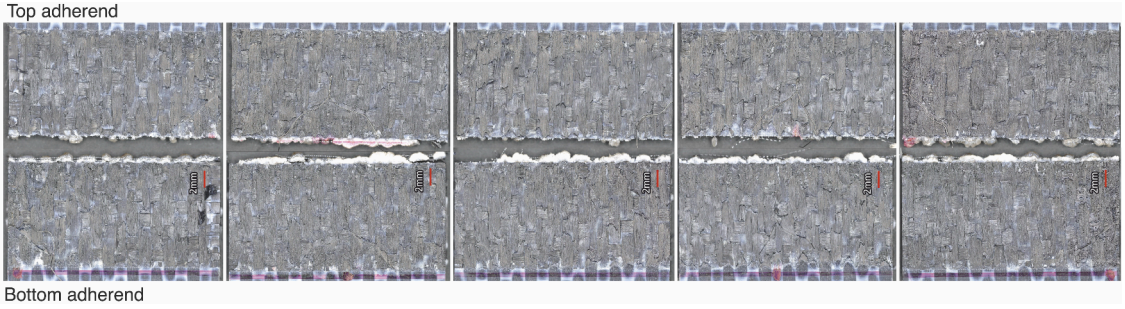

Fig. 7. Fracture surfaces of continuous ultrasonic weld made using rounded sonotrode. Welded in the direction left to right.

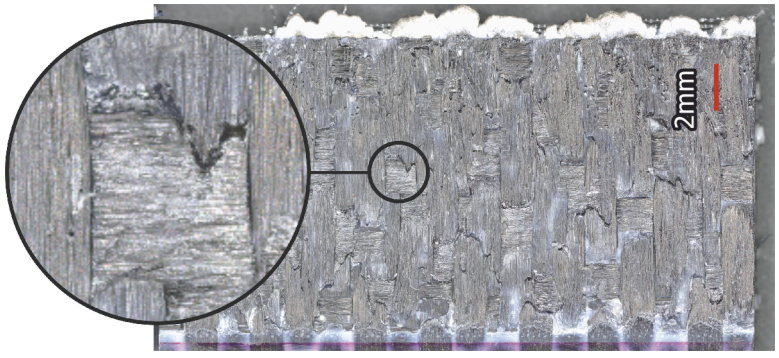

Fig. 8. Fracture surface detail from Fig. 7 of continuous ultrasonic weld made using rounded sonotrode.

adherend and energy director at five different locations along the weld is shown in the graph in Fig. 9. Likewise, for the same welding conditions Figs. 10 and 11 show the temperature evolution within the top and the bottom adherends, as well as at the weld interface, at two locations along the weld.

Discussion

The results obtained in this study show that it is indeed possible to use a rounded sonotrode to weld flat thermoplastic composites and hence suggest the potential of successfully applying continuous ultrasonic welding to curved parts. The welding process, as shown in this

paper, provides fully welded overlaps (Fig. 7) featuring first-ply failure (Fig. 8) with abundant occurrence of fibre bundle breakage. This, as acknowledged in literature, is the type of failure characteristic of high-quality welded joints in thermoplastic composites (Shi et al., 2013). It also results in adherends free from welding-induced porosity as well as minimal squeeze out (Fig. 5). Finally, the average weld strength amounts to 90% that of the highest-quality CF/PPS continuous welded joints we obtained using a rectangular sonotrode (referred to as reference continuous welds hereafter) (Jongbloed et al., 2021b) and 98% that of CF/PPS static welds (Jongbloed et al., 2022), see Table 2. Note that the reference continuous welds featured fully welded overlaps, first-ply failure and minimal material squeeze out from the adherends (Jongbloed et al., 2021b), similarly to the results shown in this paper for the rounded sonotrode (Figs. 5, 7 and 8). The reference continuous welds were obtained using the same CF/PPS material as in the present paper and a 15 mm-wide rectangular sonotrode. The process parameters were 500 N welding force, 70 μm peak-to-peak vibration amplitude, 35 mm/s welding speed and 1.6 MPa consolidation pressure (Jongbloed et al., 2021b). Note that for the experiments with the rounded sonotrode in the current study a 1000 N welding force, 80 μm peak-to-peak vibration amplitude, and 12 mm/s welding speed were used.

The present study uncovers, however, two downsides of using a rounded sonotrode. One of them is a significant decrease in welding speed, i.e., from 35 mm/s in the case of the reference welds obtained with a rectangular sonotrode (Jongbloed et al., 2021b) to 12 mm/s. This is consistent with the also significant reduction in the footprint of the sonotrode on the welding overlap, i.e., from 190 mm^2 (15 mm $\times$ 12.7 mm) to approximately 19 mm^2 (1.5 mm $\times$ 12.7 mm). A reduced sonotrode footprint accounts for a double effect on the process speed. The most straightforward one is that it reduces the area that is heated at once under the sonotrode, i.e., the heat footprint, and it therefore linearly decreases the time it takes to weld a prescribed length. Taking solely that effect into account we would predict a drop in welding speed from 35 mm/s to around 3.5 mm/s when transitioning from the 15 mm-wide rectangular sonotrode to the rounded one. However, decreasing the sonotrode footprint also has the effect of increasing the welding pressure. In this study the welding pressure was approximately 52 MPa, which was 20 times higher than the welding pressure in the reference continuous ultrasonic welding process (Jongbloed et al., 2021b). Increasing the welding pressure has been empirically shown to increase ultrasonic heat generation rates (Villegas, 2014). This second effect could hence be responsible for the welding speed in the process with the rounded sonotrode being 12 mm/s instead of just 3.5 mm/s, as predicted when only considering the reduction of the heat footprint. A decrease in the welding speed when using a rounded sonotrode is certainly a disadvantage of the process. And even though 12 mm/s is still very competitive when compared to other welding processes (Gardiner, 2022; Nicassio et al., 2022), it is expected that the speed will drop to lower values for continuous ultrasonic welding of unidirectional composite materials, given the more efficient heat dissipation provided by the unidirectional fibres (Köhler et al., 2021). The second downside is the apparent necessity to increase the welding force for the welding process to be successful, which however needs to be further investigated and understood. Increasing the requirements for the welding force is a downside since it would demand the use of heavier and more powerful robots in industrialised processes.

Opting for a rounded sonotrode comes nevertheless with some interesting advantages apart from paving the road for continuous ultrasonic welding of curved parts. Firstly, a significant decrease in the maximum temperatures registered during the welding process, from 450 °C–550 °C in the reference welds to 350 °C–400 °C (Fig. 9), which casts away potential doubts about thermal degradation risks (which we believe are, nevertheless, minimum due to the very short exposure time). More interestingly, this decrease is also observed in the temperatures measured within the adherends, which stay below the melting temperature of PPS (Figs. 10 and 11). This is also evidenced by the fact that signs of melting (in the form of deconsolidation voids in welds that did not undergo consolidation) are only observed at the weld line and adjacent layer of the top adherend in Fig. 6. Furthermore, Fig. 5 shows only a modest resin squeeze out coming out from the weld line at the edges of the overlap despite the very high welding pressure. Consequently, using a rounded sonotrode provides a solution to the substantial material (fibres and resin) squeeze-out from the top adherend identified in our previous work (Jongbloed et al., 2021, 2022) as an issue of continuous ultrasonic welding. This is an important issue since it can negatively affect the structural integrity of the adherends through phenomena such as porosity and local fibre misalignment. Finally, lower temperatures during the welding process, at the interface and, especially within the adherends, enables faster cooling to temperatures below solidification. Because of this, the requirements imposed on the consolidation block regarding position (see Jongbloed et al., 2022) and size can be relaxed. When plotting the effect of the consolidation block on temperature readings on the cooling phase (Fig. 12) one can indeed predict that a consolidator approximately half the size of the one used in this study would still deliver properly consolidated welds. Note that according to our findings in Jongbloed et al., 2022, properly consolidated welds are obtained when the consolidation pressure is applied until the temperature at the weld line has dropped below the temperature for maximum crystallization rate, which for PPS is around 170 °C (Chung and Cebe, 1992; Furushima et al., 2018).

We believe the reason why temperatures are overall lower in continuous ultrasonic welding with a rounded sonotrode is related to the time during which each location is directly under the sonotrode. Indeed taking into account the width of the sonotrode's footprint and the process speed one can see that in the process with the rounded sonotrode each location is approximately 0.16 s under the sonotrode (1.5 mm/12 mm/s), whereas this time increases to 1.6 s (15 mm/12 mm/s) in the reference case with a rectangular sonotrode. Fig. 13 shows that the temperature read by each thermocouple at the welding interface as the sonotrode first gets to their location is already approximately 300 °C and it continues to increase during all the time the sonotrode is above that location. Consequently, there is a direct relationship between the width of the sonotrode's footprint and the maximum temperature reached under the sonotrode. This is also consistent with the lower energy density and lower maximum power values measured for the process with the rounded sonotrode namely ~1.8 J/mm^2 and ~270 W compared to ~2.5 J/mm^2 and ~1140 W for the rectangular sonotrode. Finally, one might take this explanation to mean that, by significantly increasing the welding speed in continuous ultrasonic welding with a rectangular sonotrode, we should be able to obtain similar results to those obtained with the rounded sonotrode. Indeed, by increasing the welding speed in Jongbloed et al. (2021b) from 35 to 65 mm/s we did observe a decrease in the maximum temperatures reached during the welding process. However the weld strength was low and fracture surfaces did not have a uniform appearance, with the presence of unwelded areas. The reason why this does not occur in the present study might be the ability of the rounded sonotrode to provide a significantly higher and more uniform pressure due to its significantly smaller footprint and hence more uniform heat generation and higher weld quality.

Table 2
Overview of single lap shear strength values for ultrasonic welding with rectangular and rounded sonotrode.

Type of weld	Sontrode type	LSS ± stdev. (MPa)	Remarks
Continuous weld	Rounded	33.5 ± 1.4	
Continuous weld	Rectangular	37.2 ± 2.5	Taken from Jongbloed et al. (2021b)
Static weld	Rectangular	34.0 ± 1.5	Taken from Jongbloed et al., 2022

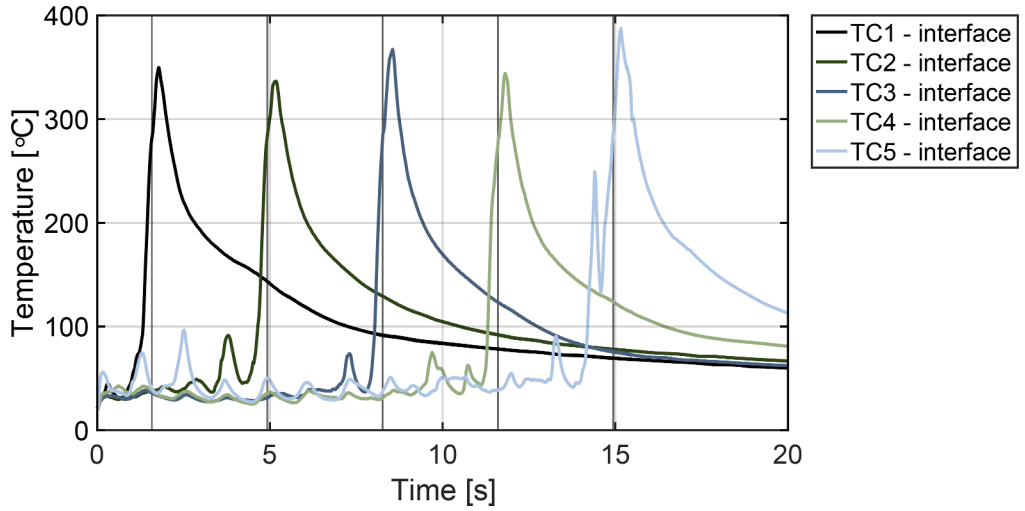

Fig. 9. Interface temperatures of continuous ultrasonic weld made with round sonotrode and the use of the consolidator. Vertical lines indicate when the middle of the round sonotrode is above the specific thermocouple.

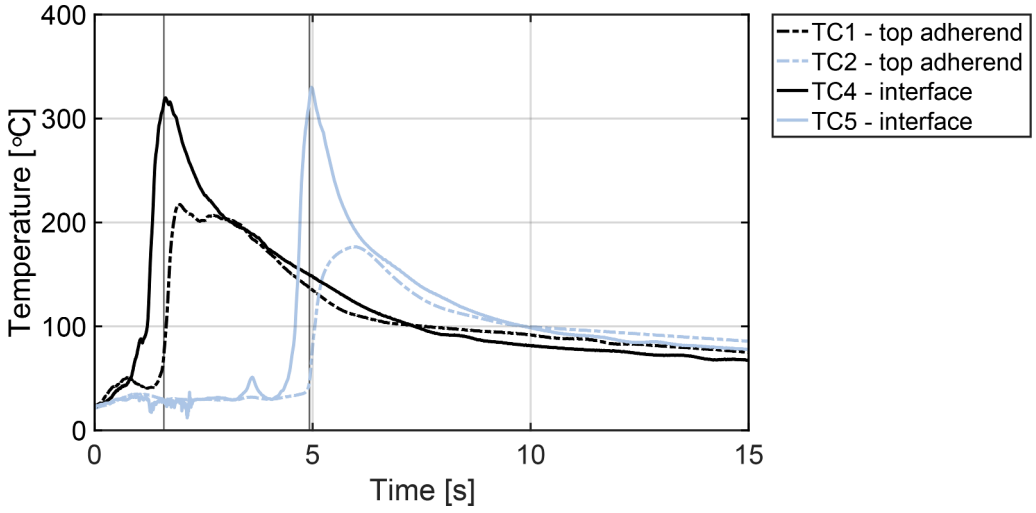

Fig. 10. Interface and top adherend temperature of continuous ultrasonic weld made with round sonotrode and with the use of the consolidator. Welding length was 78 mm. Vertical lines indicate when the middle of the round sonotrode is above the specific thermocouple.

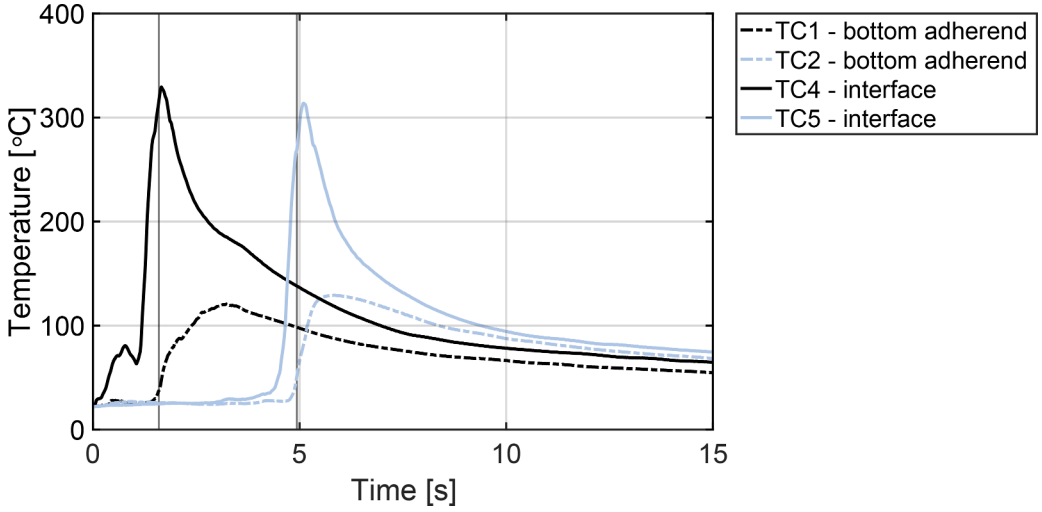

Fig. 11. Interface and bottom adherend temperature of continuous ultrasonic weld made with round sonotrode and with the use of the consolidator. Welding length was 78 mm. Vertical lines indicate when the middle of the round sonotrode is above the specific thermocouple.

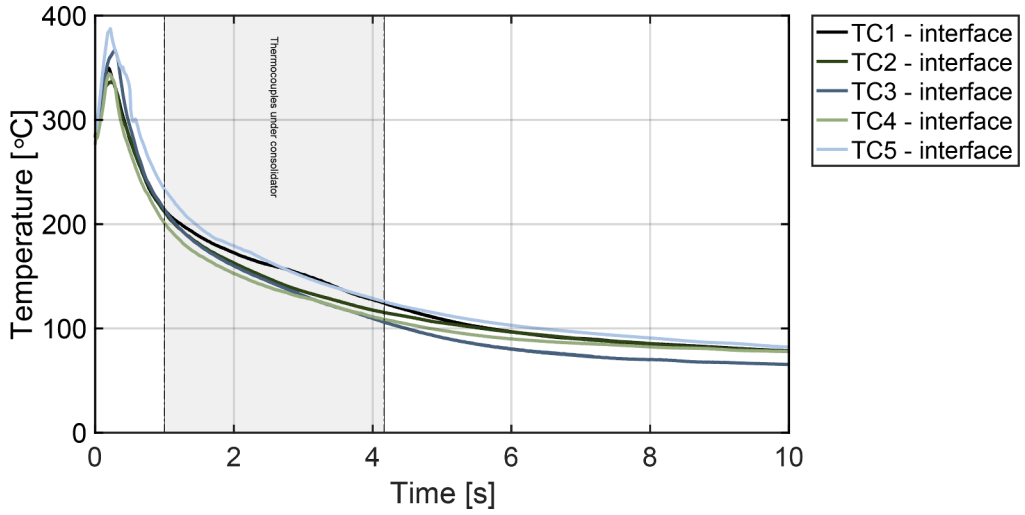

Fig. 12. Superimposed temperature profiles for the cooling phase only corresponding to the measurements shown in Fig. 9. The grey shaded area indicates the time span during which the consolidator applied the consolidation pressure.

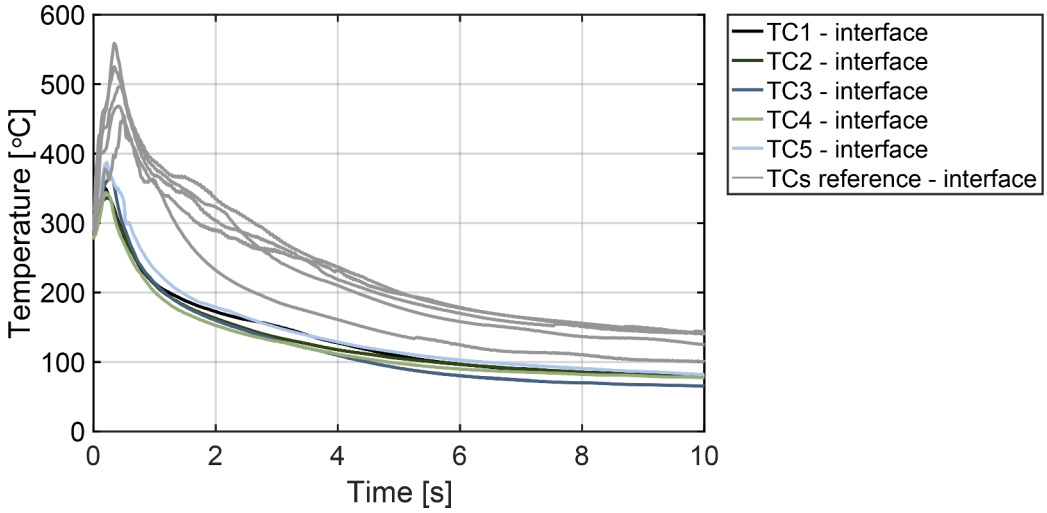

Fig. 13. Superimposed temperature profiles for the reference welds (Jongbloed et al., 2021b) and welds with a rounded sonotrode taken from Fig. 9.

Conclusions

The goal of this paper was to experimentally assess the feasibility of using a rounded sonotrode in continuous ultrasonic welding of thermoplastic composites. The main conclusions drawn from the results obtained in this research are that it is indeed possible to continuously weld thermoplastic composite panels with a rounded sonotrode and that high-quality welds can be obtained from that process. Furthermore, the use of a rounded sonotrode has the positive effect of lowering the temperatures at the welding interface as well as the temperatures within the adherends due to a shorter direct local exposure of the material to the vibrating sonotrode. As a consequence, issues that tend to occur in continuous ultrasonic welding with a rectangular sonotrode such as porosity or fibre/resin squeeze out, both of them caused by excessive bulk heating in the adherends, were eliminated in this study by using a rounded sonotrode. Furthermore, the cooling rates are faster potentially enabling the use of a smaller consolidator. As the main shortcoming the use of such sonotrode leads to a decreased welding speed, which however, thanks to a significantly increased welding pressure, was not as severe as could have been expected. All things considered, the results of this research show that using a rounded sonotrode is not only a viable but also an attractive option for continuous ultrasonic welding, which unlocks the possibility of using this process for the welding of curved thermoplastic composite structures in the future.

Declaration of Competing Interest

The authors declare that they have no known competing financial interests or personal relationships that could have appeared to influence the work reported in this paper.

Data availability

Data will be made available on reasonable request.

References

Ageorges, C., Ye, L., Hou, M., 2001. Advances in fusion bonding techniques for joining thermoplastic matrix composites: a review. Compos. - Part A 32 (6), 839–857. https://doi.org/10.1016/S1359-835X(00)00166-4.

Benatar, A., Eswaran, R.V., Nayar, S.K., 1989. Ultrasonic welding of thermoplastics in the near-field. Polym. Eng. Sci. 29 (23), 1689–1698. https://doi.org/10.1002/pen.760292311.

Benatar, A., Gutowski, T.G., 1986. Method for fusion bonding thermoplastic composites. SAMPE Q.; (United States) 18.

Chung, J.S., Cebe, P., 1992. Crystallization and melting of cold-crystallized poly (phenylene sulfide). J. Polym. Sci. Part B 30 (2), 163–176. https://doi.org/10.1002/polb.1992.090300205.

Furushima, Y., Nakada, M., Yoshida, Y., Okada, K., 2018. Crystallization/melting kinetics and morphological analysis of polyphenylene sulfide. Macromol. Chem. Phys. 219 (2), 1700481. https://doi.org/10.1002/macp.201700481.

Clean Aviation, 2022. The next generation multifunctional fuselage demonstrator—leveraging thermoplastics for cleaner skies. Retrieved from: https://www.clean-aviation.eu/the-next-generation-multifunctional-fuselage-demonstrator-leveraging-thermoplastics-for-cleaner(accessed: 24.11.2022).

Gardiner, G., 2022. Thermoplastic composites welding advances for more sustainable airframes. Composites World. Retrieved from: https://www.compositesworld.com/articles/thermoplastic-composites-welding-advances-for-more-sustainable-airframes(accessed: 24.11.2022).

Grewell, D., Benatar, A., Park, J., 2003. Plastics and Composites Welding Handbook. In: Plastics and Composites Welding Handbook. Hanser Gardener.

Jongbloed, B., Teuwen, J., Benedictus, R., Villegas, I.F., 2020. On differences and similarities between static and continuous ultrasonic welding of thermoplastic composites. Compos. Part B 203, 108466. https://doi.org/10.1016/j.compositesb.2020.108466.

Jongbloed, B., Teuwen, J., Palardy, G., Villegas, I.F., Benedictus, R., 2020. Continuous ultrasonic welding of thermoplastic composites: enhancing the weld uniformity by changing the energy director. J. Compos. Mater. 54 (15), 2023–2035. https://doi.org/10.1177/0021998319890405.

Jongbloed, B.C.P., Teuwen, J.J.E., Benedictus, R., Villegas, I.F., 2021. A study on through-the-thickness heating in continuous ultrasonic welding of thermoplastic composites. Materials 14 (21). https://doi.org/10.3390/ma14216620.

Jongbloed, B., Vinod, R., Teuwen, J., Benedictus, R., Villegas, I.F., 2022. Improving the quality of continuous ultrasonically welded thermoplastic composite joints by adding a consolidator to the welding setup. Compos. Part A 155, 106808. doi: 10.1016/j.compositesa.2022.106808.

Köhler, F., Villegas, I., Dransfeld, C., Herrmann, A., 2021. Static ultrasonic welding of carbon fibre unidirectional thermoplastic materials and the influence of heat generation and heat transfer. J. Compos. Mater. 55 (15), 2087–2102. https://doi.org/10.1177/0021998320976818.

Nicassio, F., Maffezzoli, A., Buccoliero, G., Scarselli, G., 2022. Shear buckling of aerospace panels made by induction welded thermoplastic matrix composite elements. Polym. Compos. 43 (7), 4544–4555. https://doi.org/10.1002/pc.26711.

Potente, H., 1984. Ultrasonic welding - principles & theory. Mater. Des. 5 (5), 228–234. https://doi.org/10.1016/0261-3069(84)90032-3.

Senders, F., van Beurden, M., Palardy, G., Villegas, I., 2016. Zero-flow: a novel approach to continuous ultrasonic welding of CF/PPS thermoplastic composite plates. Adv. Manuf. 0340 (September 2017), 1–10. https://doi.org/10.1080/20550340.2016.1253968.

Shi, H., Villegas, I.F., Bersee, H., 2013. Strength and failure modes in resistance welded thermoplastic composite joints: effect of fibre-matrix adhesion and fibre orientation. Compos. Part A 55, 1–10. https://doi.org/10.1016/j.compositesa.2013.08.008.

Villegas, I., 2014. Strength development versus process data in ultrasonic welding of thermoplastic composites with flat energy directors and its application to the definition of optimum processing parameters. Compos. Part A 65, 27–37. https://doi.org/10.1016/j.compositesa.2014.05.019.

Villegas, I.F., 2019. Ultrasonic welding of thermoplastic composites. Front. Mater. 6, 291. https://doi.org/10.3389/fmats.2019.00291.

Villegas, I.F., Moser, L., Yousefpour, A., Mitschang, P., Bersee, H.E., 2013. Process and performance evaluation of ultrasonic, induction and resistance welding of advanced thermoplastic composites. J. Thermoplast. Compos. Mater. 26 (8), 1007–1024. https://doi.org/10.1177/0892705712456031.

Yousefpour, A., Hojjati, M., Immarigeon, J., 2004. Fusion bonding/welding of thermoplastic composites. J. Thermoplast. Compos. Mater. 17 (4), 303–341. https://doi.org/10.1177/0892705704045187.

Zhao, T., Broek, C., Palardy, G., Villegas, I., Benedictus, R., 2018. Towards robust sequential ultrasonic spot welding of thermoplastic composites: welding process control strategy for consistent weld quality. Compos. Part A 109, 355–367. https://doi.org/10.1016/j.compositesa.2018.03.024.

Zhao, T., Rans, C., Fernandez Villegas, I., Benedictus, R., 2019. On sequential ultrasonic spot welding as an alternative to mechanical fastening in thermoplastic composite assemblies: astudy on single-column multi-row single-lap shear joints. Compos. Part A 120, 1–11. https://doi.org/10.1016/j.compositesa.2019.02.013.

Zongbo Zhang, Xiaodong Wang, Yi Luo, Zhenqiang Zhang, Liding Wang, 2010. Study on heating process of ultrasonic welding for thermoplastics. J. Thermoplast. Compos. Mater. 23 (5), 647–664. https://doi.org/10.1177/0892705709356493.